

## Design and calibration of a wind tunnel with a two dimensional contraction

J.E. Sargison<sup>1</sup>, G.J. Walker<sup>1</sup> and R. Rossi<sup>2</sup>

<sup>1</sup>School of Engineering

University of Tasmania, TAS, 7001 AUSTRALIA

<sup>2</sup>Ecole Polytechnique de l'Universite de Nantes, FRANCE

### Abstract

A low speed, open circuit, laboratory wind tunnel has been redesigned for use in turbine blade cooling experiments. The two dimensional contraction was designed using a sixth order polynomial. This paper outlines the process of design optimisation, using Computational Fluid Dynamics (CFD) to model the contraction. The parameters that were varied were the location of the point of inflection and the curvature at the contraction inlet. The optimisation was based on flow uniformity at the working section midplane, prevention of separation in the contraction and minimising the boundary layer thickness at entrance to the working section. Calibration of the wind tunnel after construction has demonstrated the value of the design process and validated the CFD predictions.

### Nomenclature

$P$	Pressure, reference pressure (Pa)
$a, b, c, d, e, f, g$	Polynomial coefficients
$h$	Contraction inlet half height-exit half height (m)
$i$	Axial distance to point of inflection (m)
$l$	Total length of contraction (m)
$\rho$	Density (kg/m <sup>3</sup> )
$\tau_w$	Wall shear stress
$u^*$	$u^* = (\tau_w / \rho)^{1/2}$
$w$	Parameter vector
$x, y, z$	Cartesian coordinates (streamwise, vertical, transverse)
$y^+$	$y^+ = yu^* / \nu$
$\alpha$	Curvature at inlet (/m)
$'$	d/dx

### Introduction

Based on evidence in current literature, aerodynamic research is poised between experimental and computation techniques. The two are closely linked and as progress is made in the development of more advanced computational fluid models, more comprehensive experimental data are required to validate the models. In the present situation a wind tunnel was remodelled for the purpose of turbine blade cooling research. The new facility is required for detailed studies of turbulent mixing processes associated with the injection of a simulated cooling jet through the wall of the working section. The data obtained will be used to improve CFD modelling of these complex flows.

Traditionally, the design of wind tunnel contractions has been based on a pair of cubic polynomials, and the parameter used to optimise the design for a fixed length and contraction ratio, has been the location of the joining point [2, 3]. The computation of flow field within the contraction has previously utilised

incompressible, inviscid flow equations and co-ordinate transformation techniques to solve the difference equations. Published, parameterised data in the form of design charts [2] are also available to avoid the need to repeat these computations, for axisymmetric contractions.

Currently, more flexibility in the design of wind tunnel contractions can be exhibited, with the use of CFD to enable rapid testing of designs to optimise contractions of arbitrary cross-section and wall profile. The use of CFD allows for the use of higher order polynomials, and non-zero curvature or slope at inlet to the contraction. However, the performance of the contraction still requires testing after construction, as the level of CFD used for this application is typically insufficient to detect the development of longitudinal vortices through the working section such as were measured by [4].

This paper describes the design of a 2D contraction with 6<sup>th</sup> degree polynomial wall profile for a wind tunnel with a square working section and its subsequent experimental validation.

### Description of the facility

The purpose of this work was to design a wind tunnel using the inlet, honeycomb and, potentially, screens of an existing facility. The working section dimensions were increased from 125 x 225 mm to 225 x 225 mm, requiring an increase in the exit area of the contraction. The contraction inlet was 1200 x 225 mm resulting in a new area ratio of 5.3. This was lower than the limit of recommended area ratios [1], and a full analysis of the design was considered necessary. The maximum velocity in the working section was 20 m/s. The original contraction length of 2 m was retained, but the profile definition was changed from a pair of cubic curves to a 6<sup>th</sup> order polynomial. The wall curvature at inlet and the location of the point of inflection in the wall profile were chosen as design parameters.

### Parameterisation of the profile

The coordinate system for the contraction profile is defined with origin on the tunnel centre line at the contraction inlet plane, and  $x$  coordinate increasing in the downstream direction. The  $y$  coordinate defines the contraction profile and  $z$  is in the spanwise direction. A sixth order polynomial was chosen to define the profile shape:

$$y = ax^6 + bx^5 + cx^4 + dx^3 + ex^2 + fx + g \quad (1)$$

The chosen profile has 7 parameters ( $a-g$ ). Five of these are specified by the inlet and outlet height, zero slope at the inlet and outlet and zero curvature at outlet. This leaves two parameters available for optimisation. These are specified by the inlet curvature and the axial position of the point of inflection relative to the contraction length. The 7 conditions defining the profile are thus:

$$\begin{aligned}
y(x=0) &= h & y''(x=i) &= 0 \\
y'(x=0) &= 0 & y(x=l) &= 0 & y''(x=l) &= 0 \\
y''(x=0) &= \alpha & y'(x=l) &= 0
\end{aligned} \quad (2)$$

where:

$h$  = inlet half height – exit half height

$\alpha$  = inlet curvature

$i$  = axial location of inflection point

$l$  = length of contraction

The conditions specified by (2) directly provide the following constants for the polynomial (1):

$$g = h; f = 0; e = \alpha/2$$

The other constants are defined by the equation:

$$Aw = B \quad (3)$$

where, for  $\alpha = 0$  for the standard case (with no inlet curvature):

$$A = \begin{bmatrix} 30i^4 & 20i^3 & 12i^2 & 6i \\ l^6 & l^5 & l^4 & l^3 \\ 6l^5 & 5l^4 & 4l^3 & 3l^2 \\ 30l^4 & 20l^3 & 12l^2 & 6l \end{bmatrix}, B = \begin{bmatrix} 0 \\ -h \\ 0 \\ 0 \end{bmatrix}, w = \begin{bmatrix} a \\ b \\ c \\ d \end{bmatrix} \quad (4)$$

The range of the variable,  $i$ , distance to the point of inflection, which gives a sensible, monotonically decreasing curve is 0.4-0.6  $l$ . Figure 1 shows that with a lower or higher value of  $i/l$ , the profile under or overshoots respectively. This was deemed to be impractical for a contraction profile. In order to optimise the shape, the optimal position of the point of inflection was determined first, and the degree of curvature at inlet was varied for this optimal design.

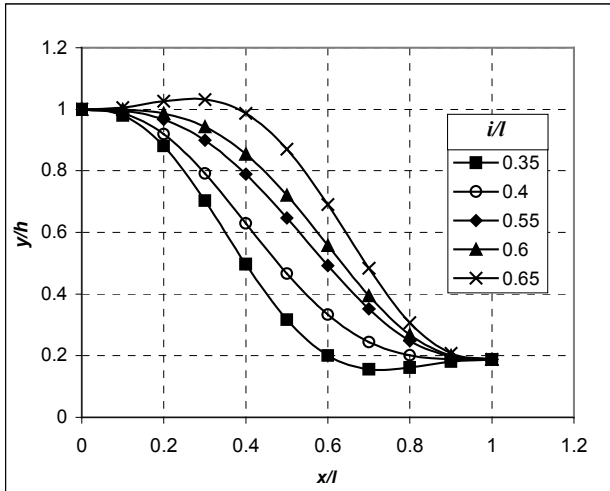


Figure 1: Contraction profiles, variation with inflection point location.

### Computational models

The commercial CFD software package CFX [5] was used to mesh, solve and postprocess the contraction model. The contraction shape was specified by the polynomial curve, with the parameter values outlined in Table 1 below. One quarter of the contraction was modelled, using the horizontal and vertical symmetry planes to reduce the size and computational load of the model. A working section of length  $0.5l$  was modelled at the end of the contraction to provide a model of the flow development beyond the end of the contraction.

Model	$i/l$	$\alpha$
1	0.4	0
2	0.55	0
3	0.60	0
4	0.60	+0.5
5	0.60	-0.5
6	0.60	+0.2
7	0.60	-0.2

Table 1: Parameters used in model study.

The Reynolds Shear Stress Transport (SST) model of turbulence was used with a specified turbulence level of 1%. A constant total pressure of 280 Pa above atmospheric pressure (or reference pressure) was used to define the inlet boundary condition, with a constant static pressure outlet boundary condition of atmospheric pressure. This generated a mainstream flow velocity of 20 m/s, which is typical of the maximum required of the facility. In the physical wind tunnel, a bellmouth inlet section is followed by a 50 mm length of honeycomb to straighten the flow. These flow manipulators were not modelled in the CFD analysis.

The model was meshed using an unstructured, tetrahedral mesh, with ten layers of mesh inflation (rectangular elements) on the walls. The minimum  $y^+$  value for the models presented in this paper was 10. The model geometry and mesh are shown in Figure 2. The mesh is shown on the inlet plane and on a plane downstream representing the middle of the working section.

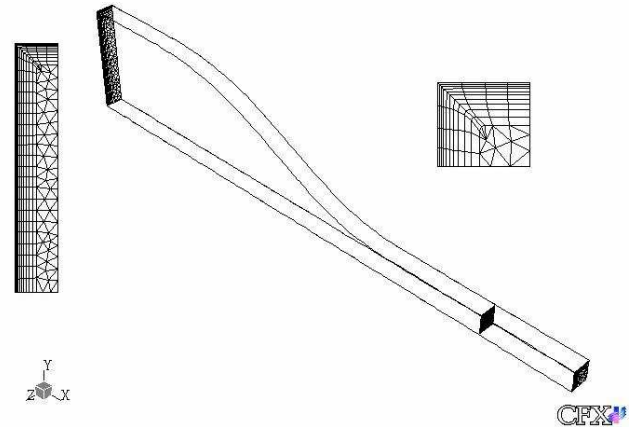


Figure 2: Model of contraction and working section, with inlet and outlet mesh (not to scale).

### Optimisation of model design

The contraction length and width were held fixed for this design, due to the existing facility geometry. The original inlet height was retained, for the practical purpose of using the existing bellmouth inlet and honeycomb. The exit height was increased compared with the existing facility in order to provide a larger working section height. This resulted in a contraction ratio of 5.3, slightly below the recommended range for an aerodynamic facility of 6-10 [1], but considered acceptable following analysis of the CFD models.

The parameters varied in the model were the location of the point of inflection, and the curvature at contraction inlet. The criteria for selection of the optimal design were maximum uniformity of the flow at mid working section (0.5m from the end of the contraction), with prevention of separation at the contraction wall.

## Computational results

The computational models were reviewed to test for uniformity of flow in the working section, and the presence of separation. It was found that none of the models tested experienced separation. In Figure 3, a typical wall shear plot for model 3 ( $i/l = 0.6$ ) demonstrates the lack of separating flow (indicated by positive values of wall shear over the entire wall).

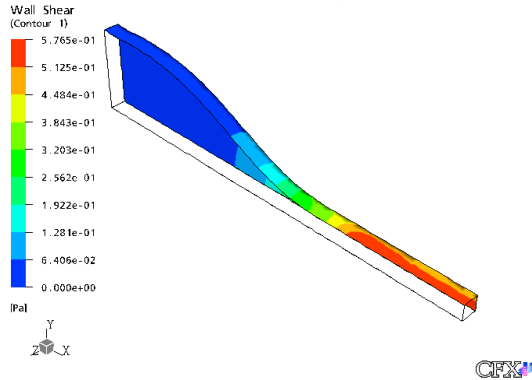


Figure 3. Wall shear (Pa), model 3.

The uniformity of the flow was compared at the mid working section shown as a shaded plane in Figure 2. The velocity profiles at this plane are shown in Figure 4. All models demonstrated reasonably uniform flow across the wind tunnel mid plane, but models 3, 5, 6 and 7 appeared to have a more uniform velocity profile. Comparison of the flow development through the working section, demonstrated model 3 to have the most uniform flow of these four models, and hence it was selected for manufacture. This profile has  $i/l = 0.6$ , and  $\alpha=0$ .

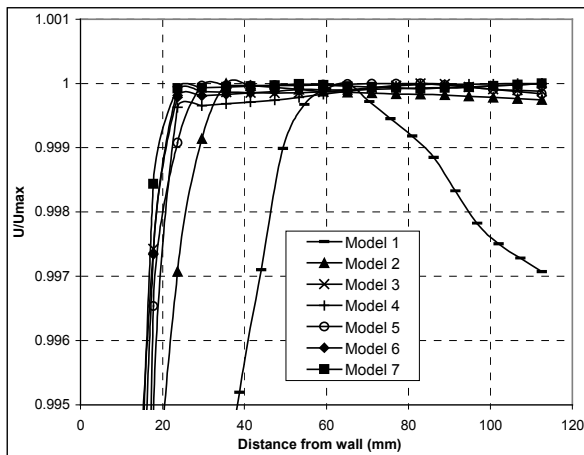


Figure 4: Velocity profile at mid working section on horizontal plane.

## Physical calibration of the facility

Following construction of the optimal design (model 3, Figure 5), experimental measurements were conducted to verify the CFD model and calibrate the facility. Calibration measurements included time mean flow, wall shear stress, flow direction and streamwise turbulence intensity in the working section. The boundary layer was tripped using a 3 mm diameter wire, 200 mm upstream of the start of the working section, in order to obtain a stable, turbulent boundary layer on all walls of the working section. Before the trip wire was installed, the boundary layer was intermittent on the side walls and laminar on the floor and top wall of the working section, resulting in a non-uniform wall shear stress distribution on the working section walls.

The mid plane of the working section was traversed with a 1.6 mm diameter pitot probe to determine the uniformity of the flow in the working section. A wall tapping in the plane of the pitot tube was used to measure static pressure, and reference static

pressures P1 and P2 were measured at the start and end of the contraction, respectively. The nominal working section flow speed was 20 m/s and Reynolds number based on working section width and flow 30 000, the maximum for the facility and equal to the flow speed obtained in the CFD analysis. The pressures were measured to  $\pm 0.005$  Pa using a Furness FC012 micromanometer, with a Furness FCS421 pressure scanner to measure the total and static pressures in differential mode (relative to P1 or Pstat).



Figure 5: Wind tunnel as constructed.

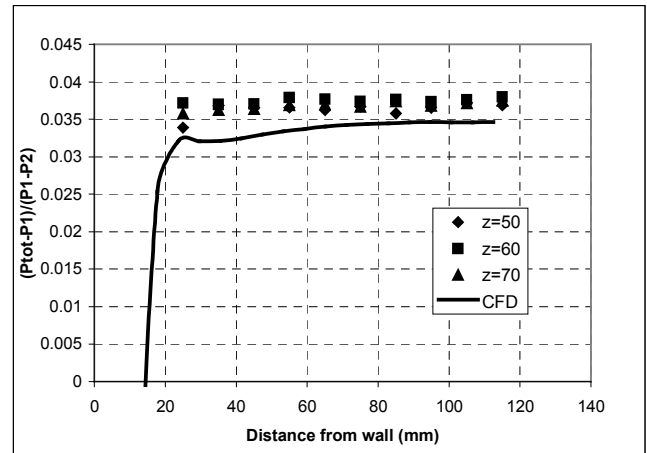


Figure 6: Pressure coefficient at mid working section measured on vertical lines.

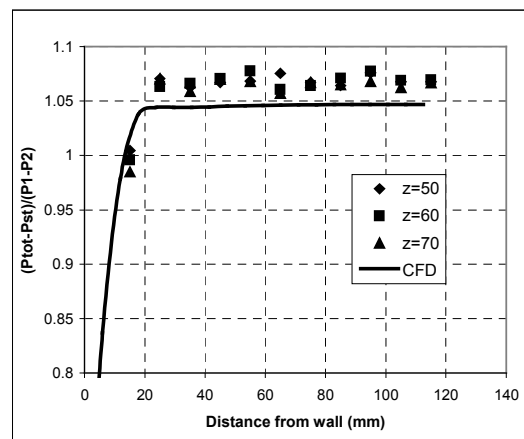


Figure 7: Relative velocity at mid working section measured on vertical lines.

Figures 6 and 7 compare the profiles of pressure coefficients and relative velocity profile, respectively at the mid working section, with the CFD model. The total pressure was measured using vertical ( $y$ ) traverses from the floor of the wind tunnel, at a number of locations in the transverse ( $z$ ) direction in the working section mid plane. The experimental results indicate that the total pressure distribution is uniform, within the experimental

uncertainty of the measurements. The CFD underpredicts the pressure coefficients in both cases (0.004 for pressure coefficient related to P1 and 0.001 for relative velocity). The uncertainty in pressure coefficient measurements was  $\pm 0.007$  (95 %) which is greater than the variation in the experimental measurements shown in Figures 6 and 7. This may be due to the CFD overpredicting the static pressure drop over the contraction (P1-P2). The pressure P1 is higher in the CFD because the honeycomb upstream of the contraction were not modelled.

The streamwise turbulence intensity was measured using a single sensor hotwire probe (Dantec 55P11) with wire axis normal to the flow and a DISA 55M constant temperature anemometer. The hot wire probe was calibrated in situ against a pitot tube and wall static tapping. The RMS voltage measured was corrected for the electrical noise in the instrument. Traverses were made in the horizontal and vertical directions in the centre of the working section, to measure the free stream turbulence. It was expected that the turbulence would be slightly above normal levels for research wind tunnels because of the reduced contraction ratio, and the lack of screens in the inlet section. This was a design parameter of the system for the intended research application, as the inlet turbulence experienced in turbine blade cooling problems is relatively high.

The turbulence profile was found to be very uniform, as shown in Figure 8, at an average level of 0.6%. The profile was symmetric in both the horizontal and vertical planes, with the larger boundary layer thickness on the sidewalls demonstrated by the horizontal traverse results.

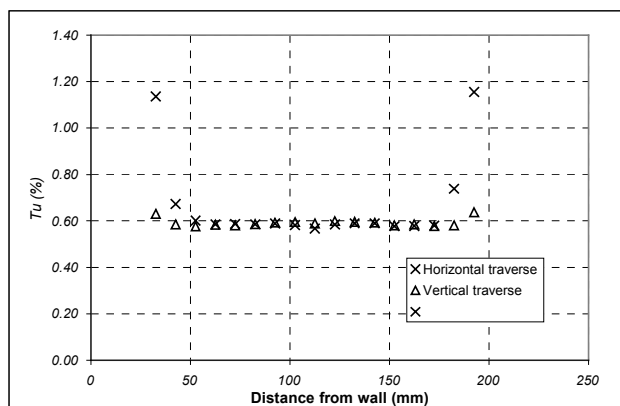


Figure 8: Turbulence profile in centre of working section.

Flow direction was measured using a three-hole probe, based on a wedge design with a rounded nose, shown in Figure 9. The probe was calibrated in a closed circuit wind tunnel. The flow direction was uniform to within  $1.1^\circ \pm 0.7^\circ$  (95%). CFD predicted a flow direction in the mid plane of maximum  $0.15^\circ$  from horizontal.

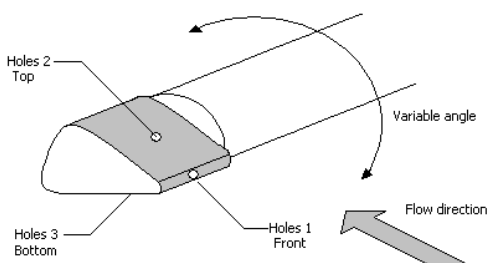


Figure 9: Three hole probe schematic.

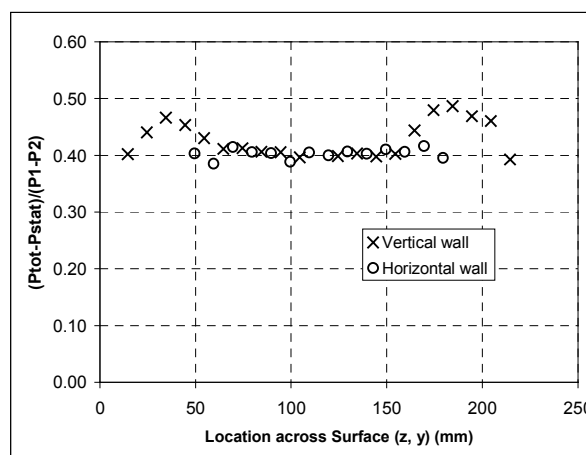


Figure 10: Development of wall shear stress with downstream distance.

Figure 10 shows the wall pressure coefficient measured using a Preston tube on the side wall and floor of the wind tunnel. The uniformity of this pressure coefficient across both walls of the wind tunnel indicates the absence of large vortices in the mainstream flow and is indicative of the uniformity of the wall shear stress in the same region. Greater secondary flow effects are evident in the corner regions on the vertical walls.

### Conclusions

CFD has been used to optimise the design of a wind tunnel contraction. The use of CFD has increased the flexibility of shapes considered, and allowed the use of a sixth order polynomial to define the profile. The parameters of the profile that were varied were the location of the point of inflection and the curvature at the contraction inlet. It was found that the best result, producing the most uniform velocity profile at inlet to the working section, and preventing separation of the flow within the contraction, was obtained when the point of inflection was located as far downstream as possible.

Physical calibration of the facility has validated the CFD methods used and demonstrated that the technique can be used for future wind tunnel designs.

### Acknowledgements

This work is supported by Rolls Royce plc, an IRGS grant from the University of Tasmania, and by the provision of an academic licence for CFX by Australian Trade Development P/L and CFX-ANSYS.

### References

- [1] Mehta, R.D. and Bradshaw, P., 1979, *Design rules for small low speed wind tunnels*, Aeronautical Journal, November 1979, 443-449
- [2] Morel, T., 1975, *Comprehensive Design of Axisymmetric Wind Tunnel Contractions*, ASME Journal of Fluids Engineering, June 1975, 225-233
- [3] Ramaseshan, S. and Ramaswamy, M.A., 2002, *A Rational Method to Choose Optimum Design for Two-Dimensional Contractions*, ASME Journal of Fluids Engineering **124** 544-546
- [4] Kim, W.J., and Patel, V.C., *Origin and Decay of Longitudinal Vortices in Developing Flow in a Curved Rectangular Duct*, Journal of Fluids Engineering **116**, 1994, 45-52
- [5] CFX user manual, ANSYS